DIAGNOSTICS OF THE LASER HEATER INDUCED BEAM HEATING IN FERMI@ELETTRA

S. Spampinati#, Sincrotrone Trieste, Trieste, Italy - University of Nova Gorica, Nova Gorica, Slovenia

S. Di Mitri, M.Ferianis, M.Veronese, Sincrotrone Trieste, Trieste, Italy

Abstract

The FERMI@elettra project [1] foresees a laser heater at low energy (~ 100 MeV); this tool has been proposed to cure the microbunching instability that affects the high brightness electron beam [2]. It consists of an undulator located in a small magnetic chicane that allows seeding of the electron beam with an external laser. The particles interact in a short undulator with the laser pulse and then gain an energy modulation on the scale of the optical wavelength. As a result, the laser-electron interaction together with the R_{52} transport term leads to an effective beam heating [3]. This article describes the capability of diagnostics dedicated to enlighten the laser heater operation.

INTRODUCTION

The laser heater is planned to be installed at the junction of the injector and of the main linac where the beam energy is roughly 100 MeV, as shown in Figure 1 [1].

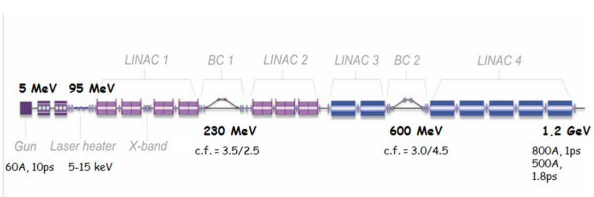

Figure 1: FERMI@elettra layout.

This device will provide a controlled increase of the uncorrelated energy spread. According to the analytical and numerical studies, the beam heating is expected to help in suppressing the microbunching instability through longitudinal Landau damping. The laser heater layout is shown in Figure 2.

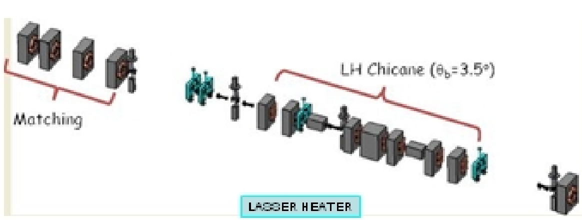

Figure 2: FERMI@elettra laser heater layout.

#simone.spampinati@elettra.trieste.it

LAYOUT

The laser heater consists of an undulator located within a small magnetic chicane that allows seeding the electron beam with an external laser. The particles interact with the laser in the short undulator and than gain a modulation on the scale of the optical wavelength. The corresponding density modulation is negligible and the induced energy/position correlation is smeared by the transverse motion in the chicane. As a result, the laser/electron interaction leads to an effective heating of the beam. The laser used for the heater will be split from the main beam of the Ti:Sa laser used for the photoinjector laser system.

The perfect heating needed to suppress microbunching instability depends on a precise laser electron alignment and overlapping and on a good undulator tuning. The relative alignment between the photon and electron beam has to be better than 50 micron rms. To achieve this, two screens, capable of recording the image of the two beams, are placed in the laser heater chicane before and after the undulator. The alignment system will be completed by a virtual laser waist and by an electron Beam Position Monitor.

The laser heater chicane is followed by the spectrometer to characterize the electron beam energy distribution. The energy spread needed from the laser heater is in the range 10 – 20 keV rms. This value is small with respect to the correlated energy spread coming from the upstream photoinjector that is in the range 60 – 300 keV rms for different values of the photoinjector RF phases. For this reason, the diagnostics dedicated to the beam heating process are quite demanding but inalienable as the laser heater needs particular attentions during the machine operation.

ENERGY MODULATION MONITOR SYSTEM

An additional dispersive section and an Optical Transition Radiation (OTR) screen placed in the laser heater chicane, just after the laser heater undulator, are sufficient to detect the beam energy modulation provided by the laser/electron interaction. The energy modulation induced at the laser wavelength is converted into a density modulation with the same wavelength. The beam density is modulated even on the harmonic of the laser wavelength [4];. Considering, as starting point, a 1D electron beam with a Gaussian energy spread and a sinusoidal energy modulation the charge density after the diagnostic chicane is [5]:

$$\rho(z) = \rho_0 + 2\sum_{n=1}^{\infty} b_n \cos(nk_l z) \quad (1)$$

$$b_n = J_n(nR_{56}k_l \frac{\Delta\gamma}{\gamma_0})e^{-\frac{\left(nR_{56}k_l\frac{\delta\gamma}{\gamma_0}\right)^2}{2}} \quad (2)$$

where is the initial charge density, k_l is the laser wave vector corresponding to the fundamental wavelength of the CTR emission, $\Delta\gamma$ is the energy modulation induced by the laser at the laser wavelength, γ_0 is the reference energy and $\delta\gamma$ is the incoherent energy spread.

The OTR screen emits coherent radiation [6] at the laser wavelength and at its harmonics**.** The emission from a bunch of N electrons is [7]:

$$\frac{dI_{bunch}^{\;2}}{d\Omega d\omega} = \frac{dI_{SingParticel}^{\;2}}{d\Omega d\omega}\left(N + N(N-1)|F|^2\right) \quad (3)$$

where $\frac{dI_{SingParticel}^{\;2}}{d\Omega d\omega}$ [6] is the single electron emission intensity, F is the form factor corresponding to the Fourier transforms of the bunch charge distribution. In first approximation F can be taken as the longitudinal form factor corresponding to the Fourier transform of the longitudinal charge distribution obtained projecting the charge distribution on the longitudinal coordinate.

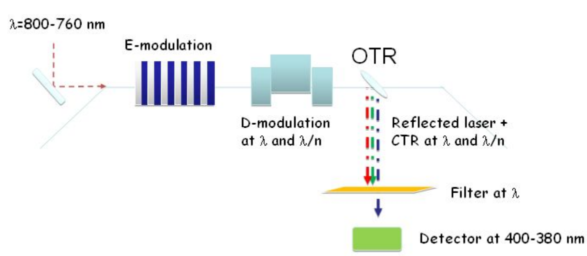

Figure 3: Layout of the energy modulation monitor system.

As the natural energy spread of the photoinjector beam is 2 – 3 keV rms only, it is possible to reach a great bunching value by properly tuning the dispersive section, even for low energy modulation. So a detectable signal can be extracted in normal operation mode without increasing the laser power.

Figure 4 shows the expected spectrum of the second harmonic of the seeding laser wavelength. Laser and electron beam transverse dimension are comparable; the energy modulation amplitude is 20 keV and the energy spread gained by the beam is 10 keV rms. The R_{56} term of the dispersive section is 0.850 mm.

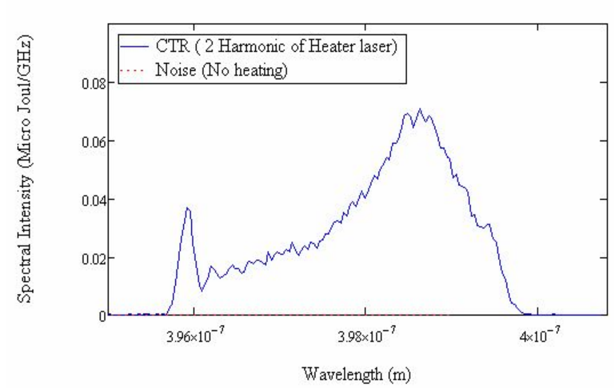

Figure 4: Spectrum of the emitted coherent transition at radiation at the second harmonic of the seeding laser wavelength.

The large bandwidth shown in Figure 4 is mainly due to the RF curvature that imposes a quadratic energy chirp to the longitudinal phase space of the electron beam. The total pulse energy is 290 μJ. The charge density distribution is provided by a particle tracking with ELEGANT code [8]

LASER HEATER SPECTROMETER LINE

One spectrometer just downstream the RF gun and another one downstream the laser heater chicane is used to measure average electron beam energy and the total energy spread [9]. The spectrometer in the laser heater area is a 45 deg, 0.5 m long bending magnet bending the 100 MeV beam towards an OTR screen. Here, the horizontal dispersion is 1 m high with a very small (~ 1 m) betatron function. Figure 5 and Figure 6 show, respectively, the layout and the corresponding optics of the spectrometer line. BPMs across the magnet and one Faraday cup complete the characterization of the beam dynamics in this region.

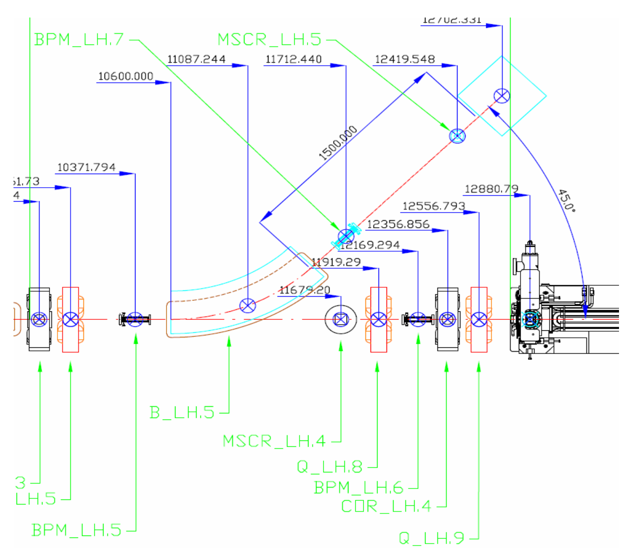

Figure 5: Layout of the laser heater spectrometer line.

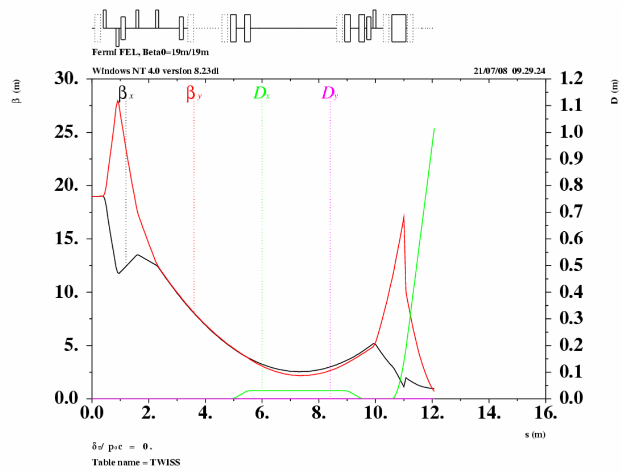

Figure 6: Optics of the laser heater spectrometer line.

LOW ENERGY RF DEFLECTOR

A low energy RF deflector is located downstream of the first magnetic compressor called BC1 [10]. Since the magnetic chicane can be switched off, another spectrometer has been added downstream the deflector to measure the slice energy spread of the electron beam after the heating process. The RF deflector converts the bunch time coordinate into vertical beam size at the downstream screen; meanwhile, the dispersive motion in the spectrometer line relates the horizontal coordinate to the particle energy. Thus, this diagnostic line allows the reconstruction of the longitudinal phase space of the beam shown in Figure 7 [9].

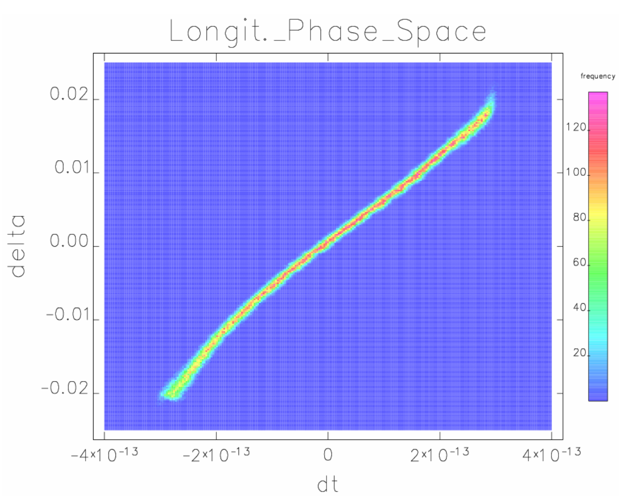

Figure 7: longitudinal phase space of the electron beam after BC1 (compressed beam).

The minimum energy difference that can be resolved at the screen is affected by the geometric contribution to the beam size and it is:

$$\frac{\Delta E_{\min}}{E} \geq \frac{2\sqrt{\beta_x \varepsilon_x}}{D_x} \quad (4)$$

Assuming 20 µm rms screen resolution, beam optics to resolve a 100 MeV uncompressed beam with 10 keV rms slice energy spread requires:

$$\frac{D_x}{\sqrt{\beta_x}} \geq 0.52 m^{1/2} \quad (5)$$

This constraint is satisfied by the current optics shown in Figure 8; it provides an rms beam size of 70 µm at the screen.

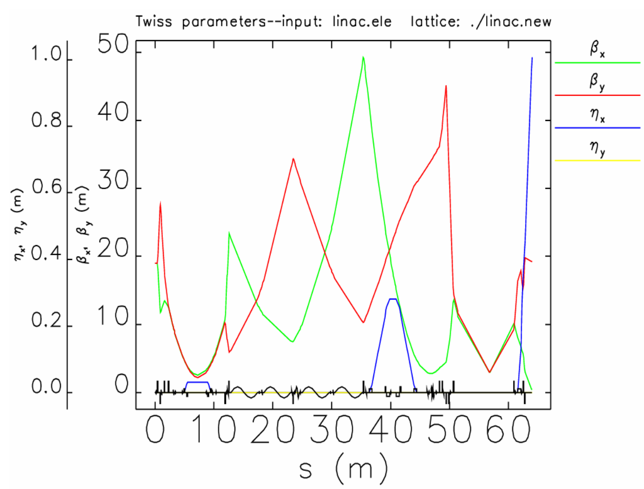

Figure 8: Optics from the injector end to the screen of the BC1 spectrometer line.

CONCLUSIONS

We have presented a possible ways to directly study the density and energy distribution of the electron beam coming up from the FERMI@elettra laser heater system.

REFERENCES

[1] C.J.Bochetta et al FERMI@Elettra cdr Trieste, Italia (2007).
[2] E.Saldin E.A. Schneidmiller, and M.V. Yurkov TESLA-FEL-2003-02, May 2003
[3] Z. Huang et al., Phys Rev ST-AB 7 074401 (2004).
[4] C.M.S.Sears et al. Prl 11 061301(2008) Sears et al
[5] E.Saldin E.A. Schneidmiller, and M.V. Yurkov TESLA-FEL-2003-02, May 2003
[6] V.L. Ginzburg, V.N. Tsytovich, Transition radiation and transition scattering
[7] O. Grimm., TESLA-FEL-2006-03, May 2006
[8] M. Borland, APS LS-287 (2000).
[9] S. Di Mitri Fermi Technical Note to be published
[10] P. Craievich at all Fermi Technical Note 07/13 September 2007.